Design of a bidirectional actuator for a nanopositioning system with a permanent magnet and an electromagnet

K. H. Kim[a] and D. G. Gweon
Nano Opto-Mechatronics Laboratory, Department of Mechanical Engineering, Korea Advanced Institute of Science and Technology, 373-1 Guseong-Dong, Yuseong-gu ME3265, Daejeon 305-701, Korea

(Received 10 September 2005; accepted 7 November 2005; published online 21 December 2005)

A precision bidirectional linear actuator for ultraprecision systems is proposed and designed in this article. The actuator is composed of a symmetric structure with a force generation unit and a guide mechanism. The force generation part consists of a permanent magnet and an electromagnet, which generate a permanent and a reversible flux, respectively. The combination of permanent and reversible fluxes makes various flux densities in its air gaps between the moving part and the fixed yokes. The difference between flux densities in the lower and upper gaps creates forces for bidirectional linear motions of hundreds of micrometers. As a guide mechanism, two circular plates and one shaft are used. Reducing other forces generated by motions, except the z-directional motion, these circular plates in the form of a flexure endow the actuator with smooth motion, freedom from wear, and a high stiffness for a rapid settling time. The function of the shaft is to transfer motion to an object. Finally, the total body has a symmetric structure enabling it to be stable in terms of thermal error. The actuator is designed with the software tools MAXWELL™2D and PRO-MECHANICA™. The designed actuator is evaluated with a linear current amplifier, a laser Doppler vibrometer for nanometer resolution, a dynamic signal analyzer for frequency responses of the proposed actuator, and a simple proportional-integral-derivative controller for its tracking performance. © *2005 American Institute of Physics.* [DOI: 10.1063/1.2148999]

I. INTRODUCTION

In our time, with the rapid development of information technology, the needs for a precision manufacturing and measuring system have increased. The precision systems need to have three-axis leveling motions $Z\theta_x\theta_y$ as well as three-axis plane motions $XY\theta_z$ in hundreds of micrometers to handle workpieces, tools, and probes.[1] These specifications are especially needed in a photolithography system, which has an optical system of a deep ultraviolet light source with a 100–300 nm wavelength and a high numerical aperture (NA) of about 0.5, with its usable depth of focus (UDOF) below the submicrometer level due to its manufacturing and its measurement of approximately 100 nm linewidth. Due to the fine UDOF, an ultraprecision stage is required such as a three-axis leveling mechanism within several tens of nanometer resolution.[2] In addition, considering the thicknesses of specimens and workpieces in biotechnology and semiconductor technology, a precision stage is required for these technologies' working ranges in the hundreds of micrometer level. The precision systems for these requirements would comprise a high-performance controller, a high-repeatability sensor, and a precision actuator. Currently, there are many studies concerning precision actuators. There are already many precision actuators found in industrial fields and in engineering fields as well.[3,4] Lead zirconate titanate (PZT) is a good example of a precision actuator for ultraprecision systems. PZT is found in a high-precision six-axis stage, with its working range in the several tens of micrometer.[5] However, PZT needs a large and complex amplification mechanism or has to have a 100 mm length to realize an ultraprecision system with a working range above 100 μm.[6,7] In addition to PZT, there are electromagnet actuators such as the voice coil motor (VCM) and solenoid. The actuators have motions without backlash and mechanical hysteresis.[8] The VCM of electromagnet actuators is generally used in precision stages of a specimen transfer mechanism and data storage.[9–11] A solenoid actuator generally has a one-direction attraction force caused by an electromagnet from its base level with a low electromechanical time constant and a nonlinear motion in millimeters.[12] Due to its restrictive mechanism, the use of a solenoid actuator is not suitable in precision systems, unlike the use of the VCM. In other words, solenoid actuators have mainly been used in many industrial areas except in precision systems, such as in a switch. An exception to this is the fact that a one-direction attraction solenoid found to be feasible in a precision leveling system with a tens of micrometer working range.[13,14] To solve their limitations, however, a few researchers have studied solenoid linear actuators.[15,16] However, the findings of these investigations show that they are not for a precision system because of the system units and characteristics involved, such as those guide mechanisms with many uncertainties. In addition, magnetic suspension systems with nonlinear characteristics between the control input and the displacement are also used in precision leveling systems. In those, Trumper *et al.*[17] and Mittal and Menq[18] suggested a geometric feedback linearization with a nonlinear (accelera-

[a]Electronic mail: khkim12@kaist.ac.kr

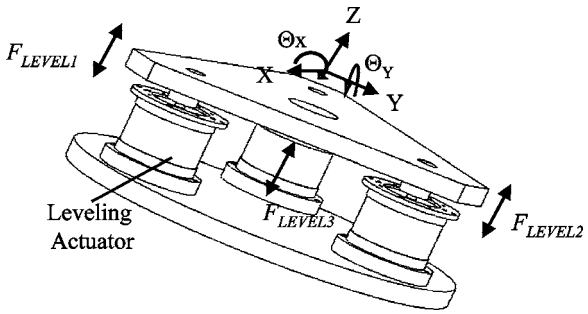

FIG. 1. $Z\theta\times\theta y$ mechanism with bidirectional actuators

tion and position) compensator to apply the linear control input (current) to suspension actuators. Particularly, Trumper introduced an experiment system with a flexure system to minimize five uncontrolled degrees of freedom (DOF's).

To settle the problems of the solenoids, this article suggests a precision bidirectional linear actuator with a flexure guide mechanism and a moving magnet and coil. The following section explains the structure, characteristics, and working principle of the proposed precision actuator. Following this, the actuator is designed with analytical equations and finite element method (FEM). Finally, the actuator is experimentally evaluated.

II. CONCEPTUAL DESIGN OF THE ULTRAPRECISION BIDIRECTION ACTUATOR

A. Design specifications

An ultraprecision system, here used in a leveling system, is shown in Fig. 1. The proposed actuator for the leveling system is designed to satisfy the following requirements of a deep-ultraviolet (DUV) photolithography system. Its wavelength (λ) and NA are assumed to be 248 nm and 0.54, respectively. In that case, the UDOF may be described as in Eq. (1).[19]

$$\mathrm{UDOF} = 0.5\frac{\lambda}{\mathrm{NA}^2} \approx 700\ \mathrm{nm}. \tag{1}$$

In addition, considering a $25\times 36\ \mathrm{mm}^2$ specimen handled by a manufacturing and measuring equipment, the allowable titling angle of the leveling system is described as in Eq. (2). As a result, the proposed actuator should have a performance of about 50 nm resolution, one tenth of the required performance.

$$\phi_{\mathrm{tilt}} \approx 0.5\frac{\lambda}{\mathrm{NA}^2 D_{x,y}} \approx 19\text{–}28\ \mu\mathrm{rad}, \tag{2}$$

where $D_{x,y}$ is the length of a specimen.

The thickness of an organism and of a micromachined product may be in the several hundreds of micrometer. For a precision system to handle this, the proposed actuator needs to have a stroke of around 200 μm (±100 μm). In addition, to perform a rapid settling below 0.1 s with a fixing part of a chuck, of which the mass is approximately 1 kg, an actuator with a natural frequency higher than 50 Hz is required.

As mentioned above, a solenoid generally has a one-directional motion and low dynamic characteristics. A solenoid consists of an electromagnet and a reversal mechansm

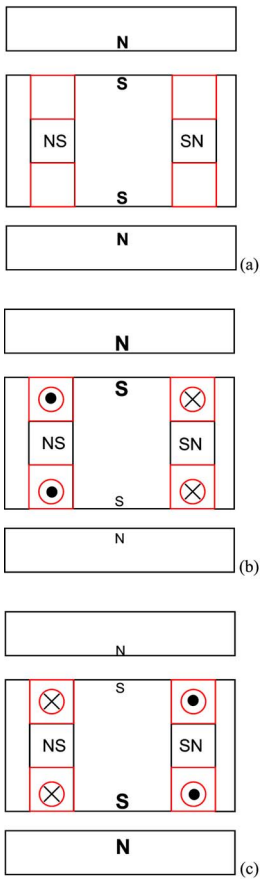

FIG. 2. (Color online) Schematic of bidirectional actuation system: (a) without current, (b) with clockwise current, and (c) with counter clockwise current.

using coil springs. The solenoid makes only a one-directional attraction force caused by its electromagnet. Returning to its initial position, the reversal mechanism is operated in solenoids. This operating mechanism makes solenoids slow and unstable in their motion. Due to the mechanism with the coil springs, solenoids especially have drawbacks in the making of high-precision movements.

The proposed actuator consists of an actuation unit with a permanent magnet, electromagnets, and a flexure guide mechanism with circular plates. The actuation unit gives the actuator bidirectional forces. In contrast to a general solenoid, at a returning motion the bidirectional force adds a returning force to its reversal mechanism, the flexure guide mechanism. The flexure guide mechanism allows the bidirectional actuator to have a smooth motion and to be free of wear. In addition, its high stiffness makes the actuator capable of a rapid dynamic movement. In the results, the proposed actuator with the bidirectional force and circular plates obtain a faster movement and a higher precision mechanism.

B. Principle of the actuation force

The bidirectional actuation system consists of a permanent magnet, an electromagnet by coils, and closed yokes. The actuation principle is conceptually described in Fig. 2. Without an electrical current, the actuation system in the center position has no motion, as shown in Fig. 2(a). Applying a clockwise current, a virtual magnet is added to the upper side

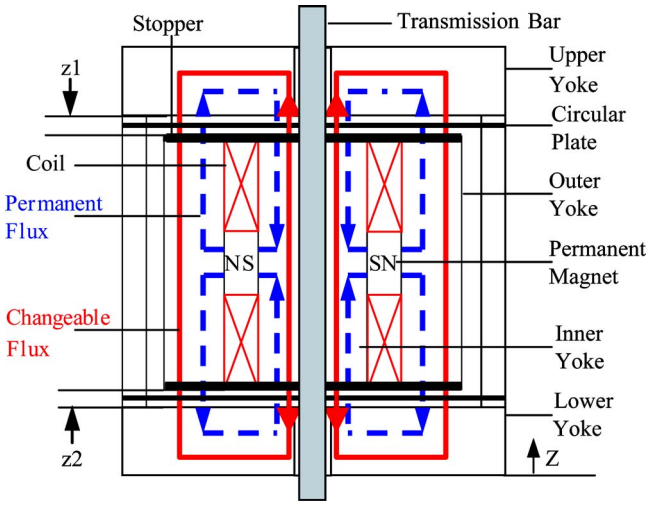

FIG. 3. (Color online) Sectioned schematic of the proposed actuator.

of the actuation unit, as shown in Fig. 2(b). With the addition of the virtual magnet, the actuator has an upward motion. Applying a counterclockwise current, a virtual magnet is created in the lower side of the actuation unit, as shown in Fig. 2(c). This time, the actuator has a downward motion. However, in a general solenoid with no permanent magnet or currents being induced, the actuation system has no motion at the initial position, at which the thicknesses of the gaps are the same.

The principle of the bidirectional actuator is concretely represented in Fig. 3. The symmetric dotted lines of the constant fluxes $\phi_{\text{permanent}}$ are generated by the permanent magnet and the closed yoke system. The direction of the constant flux depends on the relation between the gaps and the closed yoke system. Following this, inducing currents to the coils without the constant magnetic flux, solid lines in Fig. 3 represent the reversible fluxes ϕ_{change}. The magnetic fluxes in the gaps, $z1$ and $z2$, are described in Eq. (3). Forces $F_{\text{gap\_}z1,z2}$ in the gaps in Eq. (4) happen due to the change of the flux linkages. The difference of the forces in Eq. (5) is especially controlled and changed due to the direction of the current through the coils. The forces may be linearized in a small working range in approximately hundreds of micrometer range. The linearizations will be explained in the following sections with the simulation results.

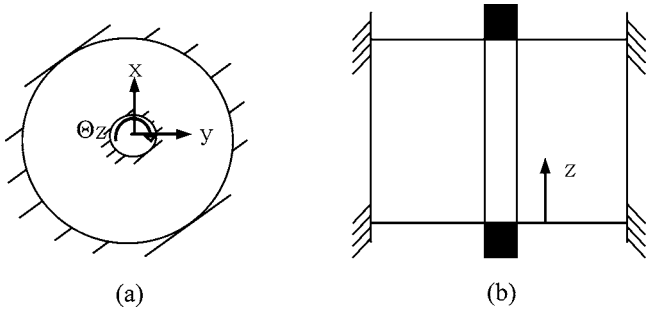

FIG. 4. Flexure guide mechanism: (a) clamped circular plate and (b) the assembly of shaft and circular plate.

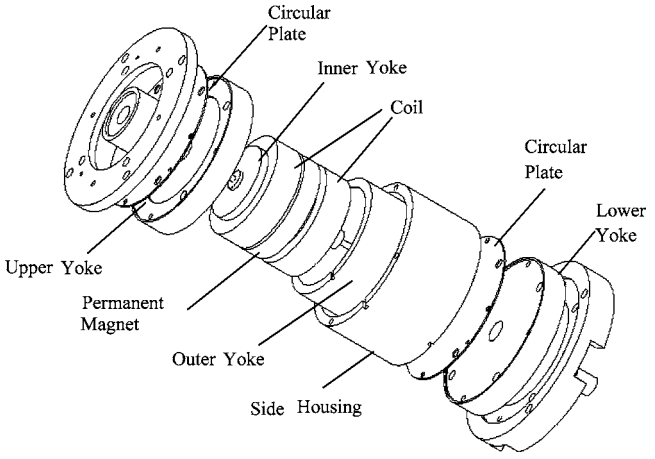

FIG. 5. Schematic of symmetric cylinder bidirection actuator.

$$\phi_{\text{gap\_}z1,z2} \approx \phi_{\text{permanent}}\left(\frac{A_{\text{gap}}l_m}{A_{\text{magnet}}z + A_{\text{gap}}l_m}\right) \mp NIP_{\text{gap1,2}}, \tag{3}$$

$$F_{\text{gap1,2}} = \frac{1}{2}\frac{\phi^2_{\text{gap1,2}}}{A_{\text{gap}}\mu_0}, \tag{4}$$

$$F = F_{\text{gap1}} - F_{\text{gap2}}, \tag{5}$$

where $P_{\text{gap1,2}}$ are the permeances of the gaps and l_m is the length of the permanent magnet.

The actuation unit needs a guide system to transfer forces from an actuating part to a specimen. In a nanometer scanning system, the frictionless, no-wear, and smooth guide mechanism of a flexure is essentially needed.[20] The proposed actuator may be used in an ultraprecision system for an ultrafine resolution limited by a sensor and a servo controller with a stroke of hundreds of micrometer. The actuator should especially be able to confer a rapid movement on a specimen. With the bidirectional force to be created by the pro-

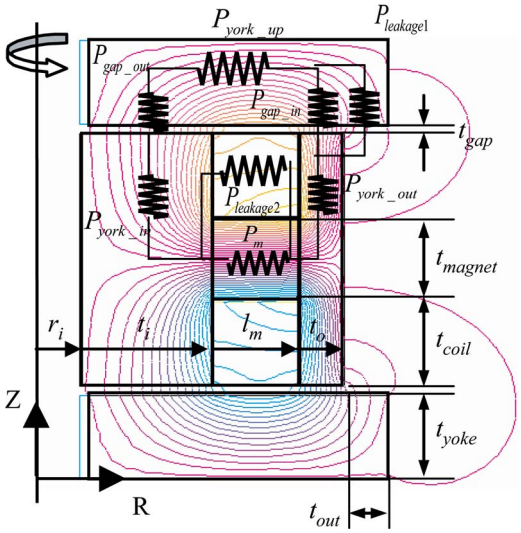

FIG. 6. (Color online) Sectioned model without current in coil in cylindrical coordinate using MAXWELL™2D.

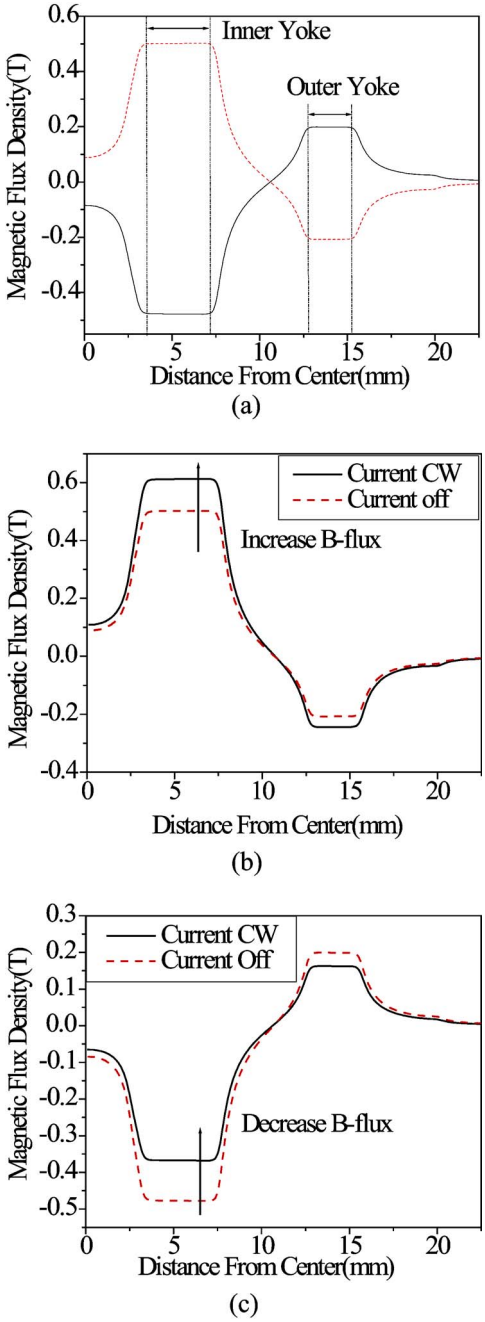

FIG. 7. (Color online) Flux densities in lower and upper gaps: (a) Initial state, (b) upper gaps with clockwise current, and (c) lower gaps with clockwise current.

posed actuation system, the requirements are accomplished with the flexure guide system with circular plates as shown in Fig. 4.

Finally, the symmetric mechanisms, as shown in Fig. 5, are applied to the proposed actuator for solving problems due to tolerance of assembly, heat dissipation, and other factors. To maintain its symmetric structure, the components are similar in shape to a doughnut or cylinder. While in this shape, its moving parts, consisting of coils, a permanent magnet, a transmission bar, and an inner yoke, are in motion with other components of the bidirectional actuation unit.

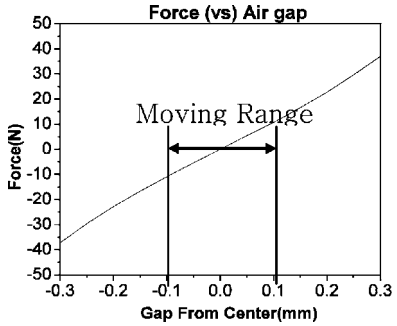

FIG. 8. Force variation according to the variance of the gap by a permanent magnet.

III. DESIGN OF THE PRECISION BIDIRECTION ACTUATOR

In this section, the actuation unit and circular plates are conceptually designed with permeances for magnetic fluxes by the permanent magnet, the electromagnet, and the mechanical stiffness of the clamped circular plates. In sequential trial and error with a FEM, the design of the proposed bidirectional actuator is concluded according to the relations between design specifications and the components of a required actuator.

With the assumption that the moving part is initially located at the center of the actuator to obtain magnetic flux and forces in the gaps, we use the permeances of Eqs. (6)–(13) along with Eqs. (3)–(5).[21,22] The permeances are selected from among many permeances represented in a magnetic-flux-line model, as shown in Fig. 6. As a result, diameters and thicknesses of outer and inner yokes are 15 and 31 mm and 5 and 3 mm, respectively. There is about a 0.5 T flux density in the initial gap of the inner yoke; however, the flux density by the permeance method is the averaged data in the air gaps.

$$P_m = \frac{\mu_m A_m}{l_m}, \quad A_m = 2\pi\left(r_i + t_i + \frac{l_m}{2}\right)t_{\text{magnet}}, \tag{6}$$

$$P_{\text{yoke\_in}} = \frac{\mu_{\text{yoke}} A_{\text{yoke\_in}}}{t_{\text{coil}} + t_{\text{magnet}}/2}, \quad A_{\text{yoke\_in}} = 2\pi\left(r_i + \frac{t_i}{2}\right)t_i, \tag{7}$$

$$P_{\text{yoke\_out}} = \frac{\mu_{\text{yoke}} A_{\text{yoke\_out}}}{t_{\text{coil}} + t_{\text{magnet}}/2},$$

$$A_{\text{yoke\_out}} = 2\pi\left(r_i + t_i + l_m + \frac{t_o}{2}\right)t_o, \tag{8}$$

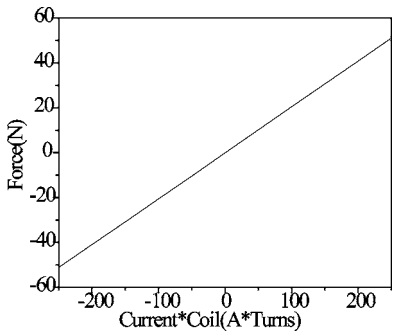

FIG. 9. Force variation according to the variance of the current.

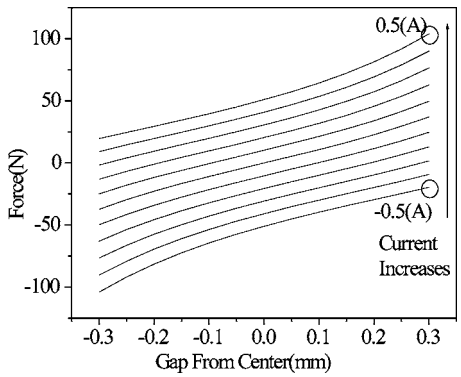

FIG. 10. Force variation according to the variance of the gap and current with a permanent magnet.

$$P_{\text{yoke\_up}} = \frac{\mu_{\text{yoke}} A_{\text{yoke\_up}}}{t_o/2 + l_m + t_i/2},$$

$$A_{\text{yoke\_out}} = 2\pi\left(\frac{r_i + t_i + l_m + t_o}{2}\right) t_{\text{yoke}}, \tag{9}$$

$$P_{\text{gap\_in}} = \frac{\mu_{\text{air}} A_{\text{air\_gap\_in}}}{t_{\text{gap}}}, \quad A_{\text{air\_gap\_in}} = 2\pi\left(r_i + \frac{t_i}{2}\right) t_i, \tag{10}$$

$$P_{\text{gap\_out}} = \frac{\mu_{\text{air}} A_{\text{air\_gap\_out}}}{t_{\text{gap}}},$$

$$A_{\text{air\_gap\_out}} = 2\pi\left(r_i + t_i + l_m + \frac{t_o}{2}\right) t_o, \tag{11}$$

$$P_{\text{leakage1}} = \frac{\mu_{\text{air}} A_{\text{leakage1}}}{1.22 t_{\text{gap}}},$$

$$A_{\text{leakage1}} = \frac{2\pi^2 (r_i + t_i + l_m + t_o) t_{\text{gap}}}{4 \times 1.22}, \tag{12}$$

$$P_{\text{leakage2}} = 0.163 \mu_{\text{air}} \left(r_i + t_i + \frac{l_m}{2}\right). \tag{13}$$

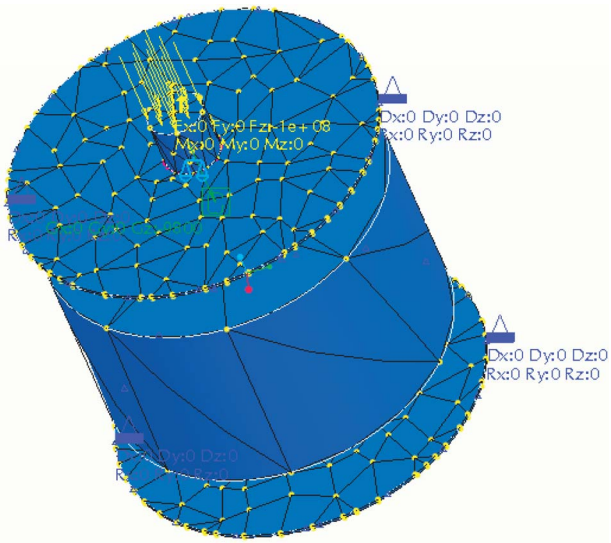

FIG. 11. (Color online) Clamping constraints for the circular plate and mesh in PRO-MECHANICA™.

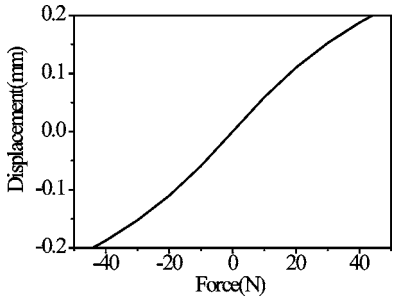

FIG. 12. Guide deflection according to the induced force to the proposed actuator.

Conversely, the characteristics of the gap flux densities are clearly obtained by FEM. With designed data by the permeance method, the electromagnet circuit for the actuating force is analyzed and designed in its symmetrical cylindrical coordinate with MAXWELL™2D, as shown in Fig. 6. The magnetic flux lines of the actuator flow through its magnetic circuit, with yokes enclosing its permanent magnet and its electromagnet. The circuit is composed of a moving part and a fixed part. The former comprises the permanent magnet, the coils for the electromagnet, and the inner and outer yokes; the latter comprises the upper and lower yokes. There is a variation of flux densities in the lower and upper gaps of the proposed actuator, with a clockwise current as shown in Fig. 7. The lower-gap flux density decreases but the upper gap increases. In other words, with the clockwise current the proposed actuator comes up.

With the design results, the characteristics of the bidirectional actuation system are analyzed as follows.

The force induced by the variation of flux densities is almost linearly changed, as shown in Fig. 8. The force of the permanent magnet can be linearized in ±0.1 mm working range. In this article, introducing a mechanical spring of $k_{\text{permanent}}$, the force $F_{\text{permanent}}$ by the permanent magnet is presented in Eq. (14)

$$F_{\text{permanent}} \approx k_{\text{permanent}} z, \tag{14}$$

where $k_{\text{permanent}}$ is approximately 0.118 (N/μm) of the system stiffness by the permanent magnet.

For an electromagnet force, current flows through the coils. Flux densities in upper and lower gaps are changed according to the direction and magnitude of the current. The variation of the electromagnet force is shown in Fig. 9. Positive and negative currents are clockwise and counterclockwise currents, respectively. The positive force is then the actuation of the actuator in a positive z direction.

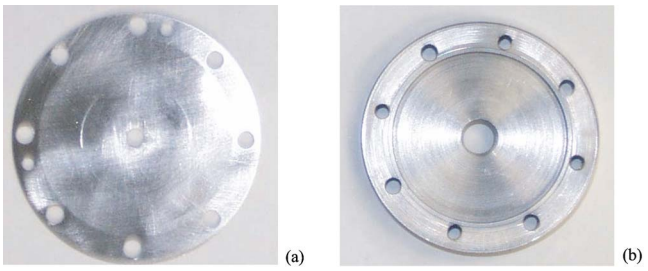

FIG. 13. (Color online) Guide plate and fixing jig: (a) circular plate and (b) upper yoke as a fixing jig.

TABLE I. The parameters of the designed actuator.

Mass (M)		330 g
Resistance of coil (R)		8.5*Ω
Number of coil windings (N)		520 turns
Coil diameter (D_{coil})		0.4 (bare)
Yoke		S10C
Permanent magnet	Material	NdFe40
	t_{mag}	4 mm
	D_{mag_in}	15 mm
	D_{mag_out}	30 mm
Circular plate	T_{cir}	0.25 mm
	D_{cir_in}	15 mm
	D_{cir_out}	40 mm

Moreover, as plainly mentioned in Fig. 7, in the combined system with the permanent magnet, when supplying current to the system the relationship of the current and gaps with the actuating force is presented in Fig. 10.

The electromagnet force is also linearized in Eq. (15).

$$F_{electro1} \approx k_{electro1} I = F_{electro}, \tag{15}$$

where $k_{electro1}$ is 106.4 (N/A) of an electromagnet force constant of the proposed actuator.

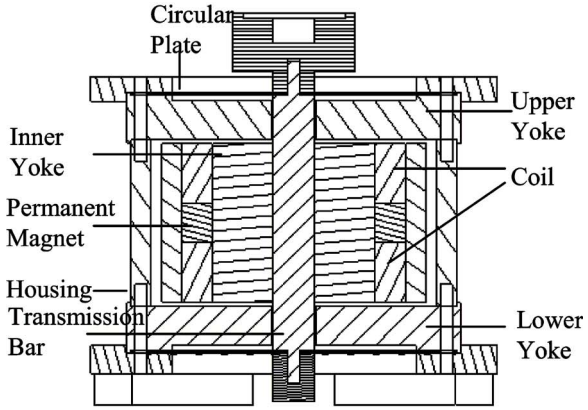

(a)

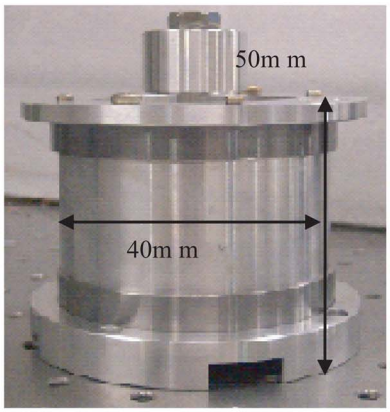

(b)

FIG. 14. (Color online) The embodied actuator: (a) The section figure and (b) the embodied actuator

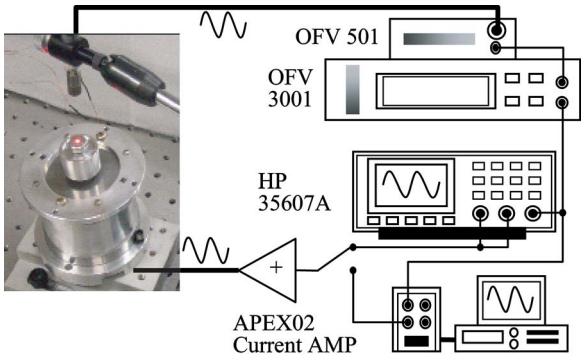

FIG. 15. (Color online) Experimental setup.

Finally, the actuating force of the bidirection actuator is presented in Eq. (16) with the current and with its motion. The motion is categorized as positive and negative in the base of the center position of the actuator.

$$F = k_{electro1} I + k_{permanent} z. \tag{16}$$

In the following section, the flexure guide mechanism design for no-wear and smooth motion is described.

Its actuating force is guided with two circular plates. At first, an approximate equation [Eq. (17)] is used to design the guide system.[23] The modal analysis for the concrete design of the circular plates in the actuator system is then carried out with PRO-MECHANICA™ using the automatic geometric element method (Auto-GEM), as shown in Fig. 11. There are 721 elements that consist of 460 tetra, 102 wedges, and 150 bricks. After repeated analyses, the circular plates made of AISI 302 stainless steel with a 0.25 mm thickness (t_{cir}), a 5 mm inner diameter (D_{cir_in}), and a 30 mm outer diameter (D_{cir_out}) are finally designed. These plates work as the flexure guide. The relationship between the induced force and the deflection of the plates is described in Fig. 12.

$$k_{cir} = \frac{8Et^3}{D_{cir\_out}{}^2[-(D_{cir\_out}/2r_i)^2/435 + (D_{cir\_out}/2r_i)/22 - 1/18]}. \tag{17}$$

Since the small stroke is about ±0.1 mm, the guide is linearly modeled in Eq. (18).

$$F = k_{cir} z, \tag{18}$$

where k_{cir} is 0.18 N/μm of the stiffness of the circular plates.

Along with Eqs. (15)–(18), the governing equation of the actuator is described in Eq. (19),

$$M\ddot{z} + k_{cir} z = k_{electro1} I + k_{permanent} z - Mg. \tag{19}$$

The designed actuator with 108 g of moving mass has the dynamic characteristic of a structural natural frequency of about 202 Hz, from Eq. (19). However, due to the force of the electromagnet and the permanent magnet, the natural frequency of the designed actuator is approximately 123 Hz.

IV. EXPERIMENTS OF THE ULTRAPRECISION BIDIRECTIONAL ACTUATOR

The bidirectional actuator is composed of yokes of low-carbon steel S10C and a permanent magnet of NdFe40. In

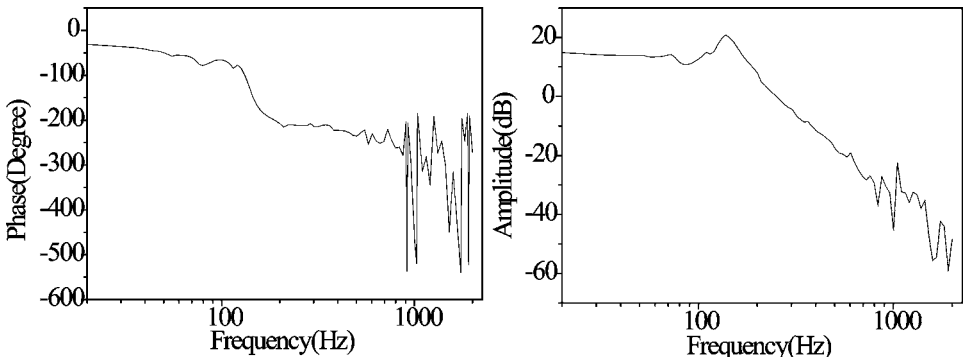

FIG. 16. Frequency response of the proposed bidirectional actuator.

addition, there are two coil parts above and below the permanent magnet, as shown in Fig. 14. The coil parts with a serial connection are made of an enameled coil with a 0.4 mm diameter. The coil parts are covered with plastic plates with a 300 μm thickness to prevent heat dissipation from being transferred to the specimen plates and to prevent the moving part of the actuator from clashing with a fixing part in an uncontrolled status. As a result of these preparations, the working range of the bidirectional actuator is limited to about ±200 μm, which is sufficient to satisfy the requirements. The two circular plates of the guide mechanism are made of an AISI 302 stainless steel with a 0.25 mm thickness and a guide shaft to transfer the force to a specimen plate of AL7075-T6 with a 5 mm diameter so as not to disturb the magnetic-flux path. The two guide plates are clamped on yokes with a shape to meet the clamping condition, as shown in Fig. 13. At the end, as mentioned above, the actuator has a symmetric cylindrical structure.The characteristics of the manufactured actuator 50 mm in height and 40 mm in diameter are described in Table I and in Fig. 14.

An experimental setup to evaluate the proposed actuator is shown in Fig. 15. The setup comprises a control system for the system performance of the tracking response and an evaluation system for the system characteristic of the frequency response function, with a 35670A dynamic analyzer manufactured by Hewlett Packard. Especially important, a sensor for the evaluation of the proposed actuator with a better range than ±100 μm has to be able to measure several hundreds of micrometers within a nanometer range for its resolution. In this article, a laser doppler vibrometer (LDV) by Polytech™, a OFV501 laser source, and a OFV3001 interface system with 8 nm resolution are used. A power amplifier, APEX PA02, is used to amplify the signals of the control system and the dynamic analyzer. With the abovementioned components, the control system of the setup comprises a 16 bit digital-analog/analog-digital (DA/AD) acquisition board of NI™, with a simple proportional-integral-derivative (PID) control scheme with 1 kHz sampling frequency.

Initially, since there is an offset due to an error in the system integration, a corresponding dc offset of 2.6 V is applied to the actuator. After the regulation, with the sine swept signal of the dynamic analyzer, a frequency response function of the actuator of about 140 Hz with approximately a 12% error from the design results is acquired (shown in Fig. 16). The error is induced by manufactured tolerances.

The working range evaluation according to the applied current is described in Fig. 17. In the results, with ±0.2 A current, the proposed actuator has about a ±100 μm stroke. These experimental results have a difference of about 10% in the comparison with the aforementioned designed results. In addition, the bidirectional actuator has nonlinear motions in the working range. Upon movement, this nonlinearity is settled with a simple PID controller in this study.

Finally, for evaluating the tracking and positioning performance with the simple PID scheme, a 50 nm, 6 Hz and a 20 μm 10 Hz sine signal are applied as references to the proposed actuator (Fig. 18). The precision bidirectional actuator has a performance below a 50 nm tracking error at the low-speed reference.

V. DISCUSSION

This article proposed a bidirectional actuator for ultrapositioning systems, e.g., a precision leveling system. For high-force and high-stiffness characteristics, the proposed actuator is composed of a bidirectional actuation unit and a flexure guide mechanism. It has a symmetric cylindrical structure. The bidirectional actuation unit consists of the constant flux of a permanent magnet, a reversible flux of electromagnets with two coils, and closed yoke structures. Its moving parts consist of a permanent magnet, two coils, an inner yoke, and a transmission bar. The flexure guide mechanism for ultraprecision positioning comprises two circular plates and a transmission bar. We used the finite element methods, the permeance method, MAXWELL™2D and permeance method for the magnetic flux analysis, and PRO-MECHANICA™ for the structural analysis to design components of the actuator. The embodied actuator has a working range of above ±100 μm, a

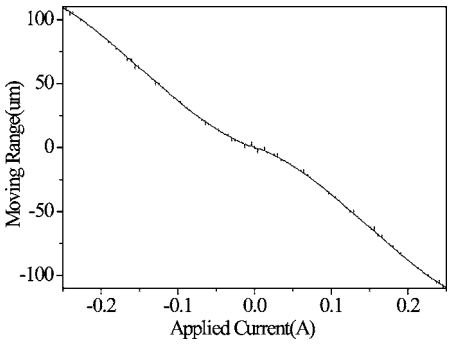

FIG. 17. The movement of this actuator due to the applied current.

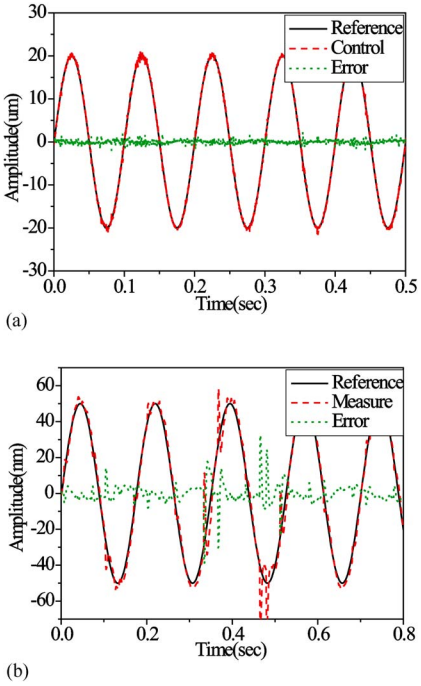

FIG. 18. (Color online) Experiment results of the linear actuator: (a) 20 μm, 10Hz sine wave and (b) 50nm, 6 Hz sine wave.

movement characteristic of 500 μm/A, and a high bandwidth of approximately 140 Hz. However, due to an error in the system integration, the actuator needed a dc offset in the region of 2.6 V and 0.15 A. In addition, the proposed actuator, with some references and simple PID, carried out a high tracking performance of approximately below 50 nm, as shown in this article.

NOMENCLATURE

λ = Wavelength of a light source (nm)
$D_{x,y}$ = Field size of x and y axis (mm)
ϕ_{tilt} = Allowable tilting range (μrad)
ϕ_{change} = Changeable flux by the activated coil (Wb)
$\phi_{\text{permanent}}$ = Permanent flux by the permanent magnet (Wb)
$z1$ = Gap between the upper fixing plate and the moving yoke (mm)
$z2$ = Gap between the lower fixing plate and the moving yoke (mm)
$\phi_{\text{gap\_}z1,z2}$ = Total flux in $z1$ and $z2$ gap (Wb)
$B_{\text{gap\_}z1,z2}$ = Flux density in the gap between fixing plate and moving yoke (T)
A_{gap} = Area of gaps (m^2)
N = Number of coil turn (turns)
$F_{\text{gap\_}z1,z2}$ = Forces in gaps (N)
F = Actuating force (N)
R = Resistance of flux linkage (A^*turns/Wb)
I = Current through the coil (A)
μ_0 = Permeability of air (H/m)
$F_{\text{permanent}}$ = Force due to permanent magnet due to the variation of air gap (N)
$k_{\text{permanent}}$ = Constant of the permanent magnet due to air gap (N/m)
F_{electro} = Force due to electromagnet due to the variation of current (N)
k_{electro1} = Constant of the electromagnet due to current (N/A)
k_{electro2} = Constant of the electromagnet due to air gap (N/m)
D_{coil} = Diameter of the coil (mm)
t_{mag} = Thickness of the permanent magnet (mm)
$D_{\text{mag\_in}}$ = Inner diameter of the permanent magnet (mm)
$D_{\text{mag\_out}}$ = Outer diameter of the permanent magnet (mm)
t_{cir} = Thickness of the guide plate (mm)
$D_{\text{cir\_in}}$ = Inner diameter of the circular guide plate (mm)
$D_{\text{cir\_out}}$ = Outer diameter of the circular guide plate (mm)

[1] W. J. Kim and H. Maheshwari, Proceedings of 2002 American Control Conference (2002), p. 4279.
[2] M. A. Van den Brink, B. A. Katz, and S. Wittekoek, Proc. SPIE **1463**, 709 (1991).
[3] A. Slocum, *Precision Machine Design* (Prentice Hall, Englewood Cliffs, 1992).
[4] D. G. Gweon, *Proceedings of The Korea-Japan Joint Symposium on Nanoengineering (NANO 2003)*, 2003, p. 192.
[5] J. W. Ryu, Ph.D. dissertation, KAIST, 1997.
[6] http://www.physikinstrumente.com
[7] J. W. Ryu, D.-G. Gweon, and K. S. Moon, Precis. Eng. **21**, 18 (1997).
[8] M. Lind, P. Kallio, and H. Koivo, *Proceedings of the Second International Conference on Machine Automation*, Tampere, Finland, 1998, p. 297.
[9] D. W. Kang, D. M. Kim, K. H. Kim, J. Y. Shim, and D. G. Gweon, *Proceedings of the ASPE 2003 Annual Meeting*, Portland, USA, 2003, p. 183.
[10] Mei-Yung Chen, Ming-Jyh Wang, and Li-Chen Fu, IEEE/ASME Trans. Mechatron. **8**, 77 (2003).
[11] J. H. Jeong, M. G. Lee, J. H. Lee, H. G. Yoon, and D. G. Gweon, Jpn. J. Appl. Phys., Part 1 **43**, 1398 (2004).
[12] Y. Mitsutake, K. Hirata, and Y. Ishihara, IEEE Trans. Magn. **33**, 1634 (1997).
[13] B. Lequesne, IEEE Trans. Ind. Appl. **26**, 848 (1990).
[14] S. A. Evans, I. R. Smith, and J. G.. Kettleborough, IEEE/ASME Trans. Mechatron. **6**, 36 (2001).
[15] S. Q. Lee and D. G. Gweon, Precis. Eng. **24**, 24 (2000).
[16] K. Harmer, G. W. Jewel, and D. Howe, IEE Proc.: Electr. Power Appl. **149**, 5 (2002).
[17] D. L. Trumper, S. M. Olson, and P. K. Subrahmanyan, IEEE Trans. Control Syst. Technol. **5**, 427 (1997).
[18] S. Mittal and C. H. Menq, IEEE/ASME Trans. Mechatron. **2**, 268 (1997).
[19] M. Born and E. Wolf, *Principles of Optics*, 6th ed. (Pergamon, Oxford, 1980).
[20] S. T. Smith and D. G. Chetwynd, *Foundations of Ultraprecision Mechanism Design* (Gordon and Breach Science, New York, 1992).
[21] A. E. Fitzgerald, C. Kingsley, and S. D. Umans, *Electric Machinery* (McGraw Hill, London, 1990).
[22] D. C. Hanselman, *Brushless Permanent-Magnet Motor Design* (McGraw Hill, New York, 1994).
[23] S. T. Smith, *Flexure* (Gordon and Breach Science, New York, 2000).